Lift Interference in Wind Tunnels with Perforated and Solid Walls

Mihaela MANEA*,[1,2], Adrian BURGHIU[1,2]

*Corresponding author
[1]INCAS – National Institute for Aerospace Research "Elie Carafoli",
B-dul Iuliu Maniu 220, Bucharest 061126, Romania,
manea.mihaela@incas.ro*, burghiu.adrian@incas.ro
[2]POLITEHNICA University of Bucharest,
Splaiul Independentei 313, 060042, Bucharest, Romania

DOI: 10.13111/2066-8201.2021.13.1.11

Received: 19 November 2020/ Accepted: 14 December 2020/ Published: March 2021

Abstract: *In order to obtain accurate results in wind tunnel testing it is necessary to determine the effect of interaction between the flow around the model and the test section walls. In this paper, the classical theory for wind tunnel wall corrections assessment is used to evaluate the wall induced change in the circulation caused by the presence of the test article in the wind tunnel. This primary correction, also known as lift interference is based on the test section geometry and it is applied to the test article angle of attack. The computations performed in this paper employ the assumption of the potential linearized flow between the test section walls and the model. As well, the principle of superposition is a key element in this analysis.*

Key Words: *wind tunnel, wall interference, lift interference, perforated wall, classical corrections*

1. INTRODUCTION

Wind tunnel wall interference manifests itself as an error in the simulation of flight conditions which occurs due to the interaction of the model flow field with the wind tunnel boundaries. Test section walls alter the flow field, thus limiting the free expansion of the streamlines. Therefore, the objective of wall interference assessment is to minimise or even eliminate the difference between the flow around a model in a uniform stream of infinite upstream, downstream and lateral extent and the flow around the same model, constrained by the test section walls.

Classical wall correction theory is based on the assumptions of linear potential flow, perturbation flow at the tunnel boundaries, a model with generally small dimensions and a wind tunnel with constant cross-sectional area extending far upstream and downstream of the model. This theory, explained in detail in References [1] and [4] involves the use of closed form equations, which are easy to implement, do not require large computational resources and lead to reliable corrections.

The upwash interference parameter δ_0 quantifies the change in average induced upwash in the vicinity of the model, which directly modifies the angle of attack. The resulted correction applied to incidence is considered to be a primary correction.

The main objective of this paper is to determine the upwash interference parameter using linear potential flow theory, in order to correct the angle of attack measured during experiments conducted in a rectangular test section wind tunnel with perforated or solid walls.

In order to achieve this, the appropriate boundary conditions describing the wind tunnel walls were defined.

Also, the compressibility effect is added by using Prandtl-Glauert compressibility factor.

2. GOUVERNING EQUATIONS

To determine the lift interference in a wind tunnel with rectangular test section, the linearized potential flow theory is used. Hence, the governing equation is

$$\frac{\partial^2 \varphi}{\partial x^2} + \frac{\partial^2 \varphi}{\partial y^2} + \frac{\partial^2 \varphi}{\partial z^2} = 0 \qquad (1)$$

Here, φ is the perturbation velocity potential function of the entire flow field, and it can be expressed at any point of the wind tunnel as the superposition of the potential due to the model and the potential due to the tunnel walls.

$$\varphi = \varphi_M + \varphi_W \qquad (2)$$

The potential due to the model is considered to be a known solution of equation (1), and, therefore φ_W can be determined by satisfying the boundary conditions at the tunnel walls.

Regarding the boundary conditions that must be satisfied at the walls, in Reference [3], Keller developed a general boundary condition of the form

$$c_1\varphi + c_2\frac{\partial \varphi}{\partial x} + c_3\frac{\partial \varphi}{\partial n} + c_4\frac{\partial^2 \varphi}{\partial x \partial n} = 0 \qquad (3)$$

The above coefficients must be specified according to the type of the wall, as indicated in Table 1.

Table 1: Values of boundary condition coefficients for different types of walls

Type of boundary condition	c_1	c_2	c_3	c_4
Closed wall	0	0	1	0
Open jet	0	1	0	0
Perforated wall	0	1	$\frac{1}{P}$	0
Ideal slotted wall: integrated form	1	0	K	0
Ideal slotted wall: differentiated form	0	1	$\frac{\partial K}{\partial x}$	K

P is a restriction parameter that must be determined experimentally, because its value varies with different test-section configurations.

3. TUNNEL WALLS AND MODEL REPRESENTATION

The wind tunnel walls are divided into rectangular elements, represented by a constant strength source distribution over the element.

If we consider that φ^* is the velocity potential function for an element divided by the source strength [3], then

$$\varphi_W = \sum_{i=1}^{N} \varphi_i^* \sigma_j' \tag{4}$$

The boundary conditions which are satisfied at the centroid of each element can be written for the four walls as in Reference [2]:

$$P\frac{\partial\varphi}{\partial x} - \frac{\partial\varphi}{\partial z} = 0 \tag{5}$$

$$P\frac{\partial\varphi}{\partial x} + \frac{\partial\varphi}{\partial z} = 0 \tag{6}$$

for top and bottom walls, and

$$P\frac{\partial\varphi}{\partial x} - \frac{\partial\varphi}{\partial y} = 0 \tag{7}$$

$$P\frac{\partial\varphi}{\partial x} + \frac{\partial\varphi}{\partial y} = 0 \tag{8}$$

for side walls. Using this method of defining for the boundary conditions, the computations can be performed even when the restriction parameter is zero ($P = 0$), as in the case of solid walls. The model is represented by lifting lines placed along the quarter chord line of the wings and the load distribution is assumed to be elliptic [2], [5]. Hence, the model can be represented by discrete horseshoe vortices distributed along the quarter chord line and described by the potentials:

$$\varphi_{M_j} = \frac{\gamma_j}{4\pi}\frac{z}{y^2+z^2}\left(1+\frac{x}{\sqrt{x^2+y^2+z^2}}\right) \tag{9}$$

The vortex strength is considered to be the area under the load distribution curve. For an elliptic load distribution, γ_j can be computed as the difference between two circular segments, constructed at the end points of the j -th interval [2]:

$$\gamma_j = \frac{1}{2\pi}\left[acos\frac{N-j}{N} - \frac{N-j}{N}\sqrt{1-\left(\frac{N-j}{N}\right)^2}\right] - \sum_{1}^{j}\gamma_{j-1} \tag{10}$$

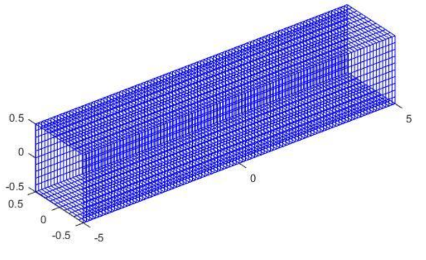

Fig. 1: Representation of wind tunnel walls

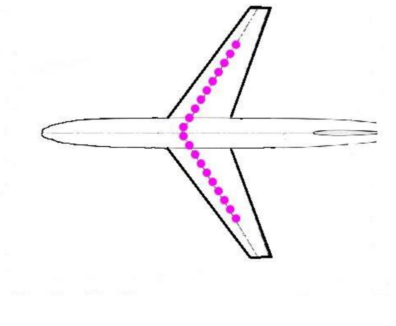

Fig. 2: Horseshoe vortices placed at the quarter chord line, used to represent the model

For the computation of source strength slopes required to satisfy the boundary conditions it is necessary to solve a matrix equation for the values of σ_j', which is used to determine the interference potential due to the tunnel walls using equation (4). The matrix equation that describes the boundary conditions has the form

$$[\mathbf{C}_{ij}][\boldsymbol{\sigma}_j'] = [\mathbf{D}_i] \tag{11}$$

where

$$\boldsymbol{C} = c_2 \frac{\partial \varphi^*}{\partial x} + c_3 \frac{\partial \varphi^*}{\partial n} \tag{12}$$

and

$$\boldsymbol{D} = c_2 \frac{\partial \varphi_M}{\partial x} + c_3 \frac{\partial \varphi_M}{\partial n} \tag{13}$$

The values obtained by solving equation (11) are then used for the computation of the upwash factor at any point of the wind tunnel.

$$\delta_0 = \frac{A}{SC_L} \frac{\partial \varphi_W}{\partial z} \tag{14}$$

$$A = B \cdot H \tag{15}$$

where B and H are the width and height of the wind tunnel test section.

After determining δ_0, the angle of attack correction, $\Delta\alpha$, is calculated as the weighted average of the interference velocity in the lifting direction. The interference is caused by the interaction between the lifting vortex and the walls. Averaging is done along the wing quarter chord.

$$\Delta\alpha = C_L \frac{S}{A} \delta_0 \tag{16}$$

In the above equation, δ_0 is a function of the model span to wind tunnel ratio, test section shape and load span distribution. Also, $\Delta\alpha$ is expressed in radians.

The corresponding corrections to the first order of δ_0 for the lift, drag and pitching moment coefficients are

$$\Delta C_L = 0 \tag{17}$$

$$\Delta C_D = C_L \Delta\alpha \tag{18}$$

$$\Delta C_M = 0 \tag{19}$$

Compressibility is taken into account by using the Prandtl-Glauert transformation. Therefore, the governing equation becomes

$$\beta^2 \frac{\partial^2 \varphi}{\partial x^2} + \frac{\partial^2 \varphi}{\partial y^2} + \frac{\partial^2 \varphi}{\partial z^2} = 0 \tag{20}$$

where

$$\beta = \sqrt{1 - M^2} \tag{21}$$

The Goethert-Prandtl-Glauert transformation [6], also used in Reference [2], assumes that y, z and φ are kept invariant, thus resulting the following compressible flow variables:

$$x = \frac{x_c}{\beta} \tag{22}$$

$$P = \frac{P_c}{\beta} \tag{23}$$

$$\delta_{0c} = \delta_0 \tag{24}$$

4. RESULTS

All calculations presented in this paper were performed for ONERA M5 model, placed in the NAE 5ft.x5ft. wind tunnel and ONERA M4R model, placed in INCAS Trisonic wind tunnel. The parameters of wind tunnel were considered to be $B = H = 1$, for convenience. The characteristics of the models are presented in Table 2.

Table 2: Parameters of wind tunnel models used for computations

Model	$b\ [m]$	b/B	S/A
ONERA M5	0.982	0.644	0.0569
ONERA M4R	0.635	0.53	0.0383

For the incompressible case, the computations were carried out for ONERA M5 model in the NAE 5ft.x5ft. wind tunnel, and the results were compared with those presented in Reference [2]. Fig. 3 and Fig. 4 show the upwash factor δ_0, as a function of t ($t = \frac{2}{\pi} atan\ P$), which in Reference [2] is considered to be more suitable for graphical displays because it varies in the range [0,1]. As it can be seen in Fig. 3 and Fig. 4, the results from this paper are in good agreement with those of Mokry, the difference between the two sets of data being of approximately 2%. The reasons for which this difference may occur, could be related to the method chosen for solving the equations or the number of rectangular elements used for the wind tunnel walls representation.

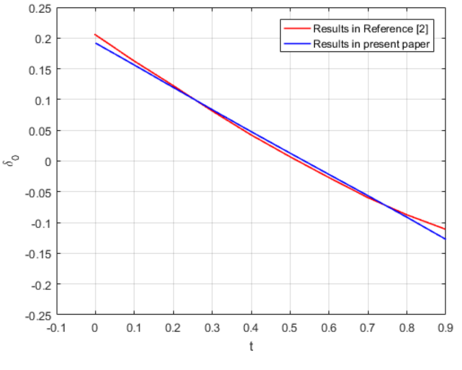

Fig. 3: Lift interference factor for ONERA M5 model-Computed at the wing tip

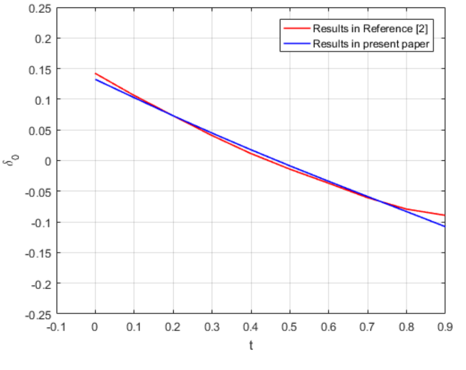

Fig. 4: Lift interference factor for ONERA M5 model-Computed at the center of load distribution

In the case of compressible flow, the computations were performed for ONERA M5 and ONERA M4R models, at 0.5 Mach, for both solid and perforated walls. The results were represented in the form of lift coefficient as a function of corrected and uncorrected angle of attack. It must be mentioned that the lift coefficient is not corrected with the effect of wall interference.

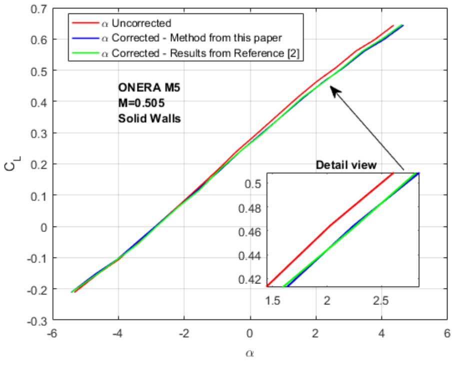

Fig. 5: Results for ONERA M5, M=0.505, Solid Walls

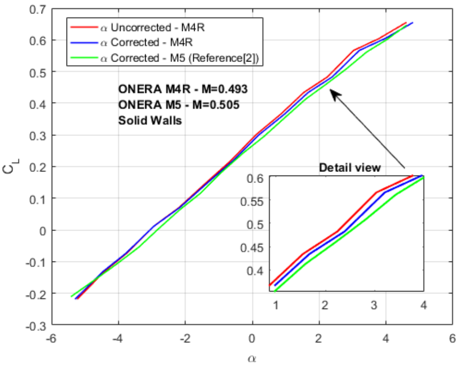

Fig. 6: Results for ONERA M4R, M=0.493, Solid Walls

From Fig. 5, we can see that the results in this paper are in good agreement with those in Reference [2]. In Fig. 6, it can be observed that even if the lift interference correction was applied to the angle of attack of ONERA M4R model, the final results do not fully correspond to the corrected ones for ONERA M5. This may arise from the existence of small differences in models geometry, wind tunnel test section configuration, flow quality, etc.

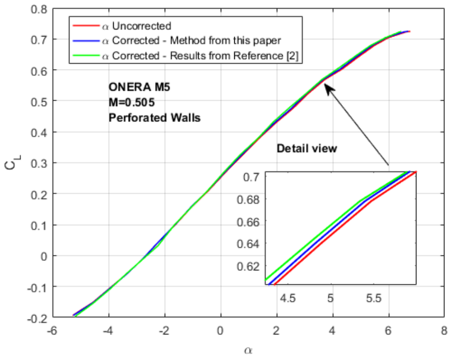

Fig. 7: Results for ONERA M5, M=0.505, Perforated walls

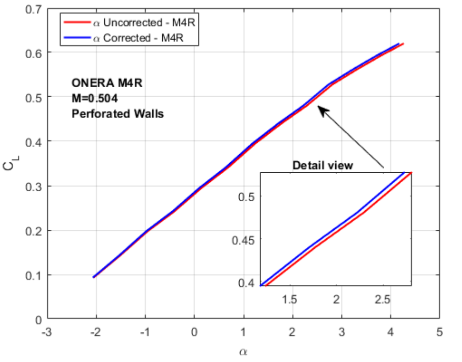

Fig. 8: Results for ONERA M4R, M=0.493, Perforated Walls

Regarding the perforated walls, it can be easily noticed, from Fig. 7 and Fig. 8 that the influence of the walls is smaller than in the case of solid walls, for both ONERA M5 and ONERA M4R. This effect is caused by the presence of the ventilated walls ($^1/_2$ inch diameter holes and an open area ratio of 20 % at NAE 5ft.x5ft. wind tunnel and 60^o inclined perforations and variable porosity at INCAS Trisonic wind tunnel), which were designed to mechanically minimize the interference in the test section.

5. CONCLUDING REMARKS

The computations performed in this paper were based on the assumption of linearized potential flow between the test section walls and the model. Appropriate boundary conditions were used, in order to simulate the perforated and solid walls of a wind tunnel. The upwash interference parameter, used to correct the angle of attack was determined for two ONERA calibration models. As it was expected, the wall interference effects were proven to be more significant for the solid walls than for the ventilated ones.

Unfortunately, this theory of wall interference assessment can provide good results only for subsonic flows, its accuracy decreasing considerably as Mach number approaches the value of 1. Also, the results can be improved if instead of an idealised boundary condition, a measured one is used. This can be achieved through wall pressure measurements and represents a more realistic characterization of the flow inside the test section.

ACKNOWLEDGEMENT

This work has been funded by the European Social Fund from the Sectoral Operational Programme Human Capital 2014-2020, through the Financial Agreement with the title (1)*"Scholarships for entrepreneurial education among doctoral students and postdoctoral researchers (Be Antreprenor!)"*, Contract no. 51680/09.07.2019 - SMIS code: 124539.

REFERENCES

[1] B. F. R. Ewald, *Wind Tunnel Wall Correction.* s.l.: AGARD-AG-336, AGARD, 1998.
[2] M. Mokry, R. D. Galway, *Analysis of Wall Interference Effects on Onera Calibration Models in the NAE 5-ft. x 5-ft. Wind Tunnel*, Ottawa: National Aeronautical Establishment, 1977.
[3] J. D. Keller, *Numerical Calculation of Boundary-Induced Interference in Slotted or Perforated Wind Tunnels Including Viscous Effects in slots*, Washington D.C.: NASA, 1972.
[4] H. C. Garner, E. W. E. Rogers, W. E. A. Acum, E. C. Maskell, *Subsonic Wind Tunnel Wall Corrections.* England: AGARD-AG-109, AGARD, 1966.
[5] J. D. Keller, R. H. Wright. *A Numerical Method of Calculating the Boundary-Induced Interference in Slotted or Perforated Wind Tunnels of Rectangular Cross Section*, Hampton: Langley Research Center, TR R-379, 1971.
[6] H. Ashley, M. Landahl, *Aerodynamics of Wings and Bodies*, Massachusetts: Addison-Wesley Publishing Company, 1965.
[7] R. D. Galway, M. Mokry, *Wind Tunnel Tests of Onera Aircraft Models*, Ottawa: National Aeronautical Establishment, 1977.
[8] F. Munteanu, *Experiments with ONERA M4R*, Bucharest: INCAS Internal Report, A-6040-1, 2012.
[9] C. Nae, *Studiul Teoretic și Experimental al Corecțiilor de Suflerie în Regim Subsonic Ridicat*, Bucharest: INCAS Internal Report, P-1495, 1994.